

Posture from Motion*

Felix Wenk¹ and Udo Frese²

Abstract—This paper presents an estimator to obtain the posture of a moving skeleton, i.e. all relative orientations of the skeleton’s bodies that are connected via a common joint. The estimator uses inertial sensor data only, the relative orientation around all axes is obtained without magnetometers. Instead, the accelerations of the skeleton’s motion provide information about the otherwise missing degree of freedom. The method also yields the orientation of the skeleton as a whole except for the heading.

In addition, a technique to decouple the estimation rate from the sensor sampling rate is introduced. The estimator both with and without rate decoupling is evaluated against ground truth data and yields relative orientations about 5 degrees off ground truth while the skeleton moves.

I. INTRODUCTION

Motion Capturing is a very popular technique to record and analyse the postures of humans over time. It appears in various fields of science, engineering and art. While the most visible application certainly is determining the postures of actors to animate characters for movies, it is also used in technically much more constrained environments.

In contrast to character animation, where postures are typically recorded by observing markers attached to the human with cameras, medical and job-safety applications are usually constrained to worn sensors. For instance, the CUELA[1] system to assess the musculoskeletal load of manual workers, uses both worn inertial and mechanical sensors to determine the worker’s postures. The system is relatively heavy weight (3kg) and not suitable for daily use by the worker.

Vignais et. al. developed a system [2] primarily relying on inertial sensors and magnetometers to determine the posture of a human, who has the sensors strapped on to his limbs. The usage of magnetometers though precludes using their system in environments with constantly changing magnetic fields.

To get closer to universal, unobtrusive applicability of posture estimation of manual workers, the sensors need to be small, possibly integrated into the worker’s cloths, such as for example in [3], and should, in contrast to [3], not rely on the environment’s magnetic field. Roetenberg et al. [4] appear to be quite successful in eliminating the magnetometer, but being a commercial product, they do not clearly say how they accomplish this.

*This work is funded by the BMBF project SIRKA (16SV6238K).

¹Felix Wenk is with the German Research Center for Artificial Intelligence, Bremen, Germany. Felix.Wenk@dfki.de

²Udo Frese is with both the Department of Mathematics and Computer Science, University of Bremen, Bremen, Germany and the German Research Center for Artificial Intelligence, Bremen, Germany Udo.Frese@dfki.de

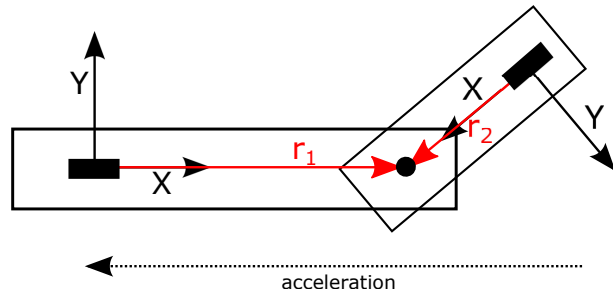


Fig. 1. Top-down view on two bodies (rectangles) connected over a joint (circle), each equipped with an accelerometer (filled rectangles). The acceleration is measured by both sensors on different axes. This is the key idea how complete relative orientation can be recovered without magnetometers.

The project SIRKA¹, which this work is part of, aims for building such miniature sensors (20mm × 20mm × 3mm) to integrate them into the worker’s usual clothing and use them to estimate their postures without magnetometers.

The main contribution of this paper is an algorithm to estimate the relative poses of the bodies of a human skeleton, i.e. the human’s posture, from inertial sensor data only, without other sensors such as magnetometers. In addition we present a technique to implement this algorithm on computationally constrained devices by decoupling the estimation from the sampling rate of the sensors.

The remainder of this paper is organized as follows. In the following Section II we explain how to obtain the posture of a skeleton from orientation estimates and most importantly our method to obtain those orientation estimates. Decoupling estimation rate from sampling rate is discussed in Section III. Our method is evaluated using the components we intend to build the sensor suit with. The results are presented in Section IV and are the basis for the conclusions drawn in the last Section V.

II. RELATIVE ORIENTATION ESTIMATION

A. Obtaining Posture from Orientation Estimates

To estimate the posture of a skeleton, the relative poses of the skeleton’s bodies that are connected via joints need to be estimated. To do so, it suffices to determine for each joint of the skeleton the orientation of the body succeeding the joint relative to the body preceding the joint (or vice versa).

If the positions $r_1, r_2 \in \mathbb{R}^3$ of the joint connecting two bodies 1 and 2 are known relative to both bodies’ origins, then the pose of body 2 relative to body 1, represented by the homogenous coordinate transform $T_{1 \leftarrow 2} \in \mathbb{SE}(3)$, can be

¹<http://www-cps.hb.dfki.de/research/projects/SIRKA>

calculated by chaining the homogenous coordinate transform

$$T_{1\leftarrow 2} = \begin{bmatrix} I_3 & r_1 \\ 0 & 1 \end{bmatrix} \begin{bmatrix} Q_{1\leftarrow 2} & 0 \\ 0 & 1 \end{bmatrix} \begin{bmatrix} I_3 & -r_2 \\ 0 & 1 \end{bmatrix}, \quad (1)$$

where I_3 is the (3×3) identity matrix and $Q_{1\leftarrow 2} \in \mathbb{SO}(3)$ the orientation of body 2 relative to body 1.

This extends to all such pairs of bodies of the skeleton, so to get the posture, only the relative orientations need to be estimated. If one also wants to know the skeleton's orientation as a whole, it suffices to estimate the orientation of a single body of the skeleton in world coordinates. Obtaining a global position requires further methods, e.g. step tracking, which are not considered here.

B. Relative Orientation Estimation without Magnetometers

Usually the orientation of a rigid body is estimated using a Kalman Filter [5], as for instance in [6], which integrates measurements from an IMU and a magnetometer, both attached to the rigid body. The gyrometer measurements are integrated to follow short-term orientation changes and the accelerometer and magnetometer measurements to correct long term errors.

The measurement model of the accelerometer is based on the assumption that on long-term average negative gravity is measured. Because gravity always points to the earth's center, this allows to determine the orientation except for the angle around the direction of gravity. This angle, the heading, is conventionally determined using the magnetometer.

To get rid of the magnetometer, known accelerations with directions different from the vertical, i.e. the direction of gravity, are needed. For this, there need to be accelerations, i.e. if the body is not moving at all, there's no way to get heading information out of the accelerometer. Even if the single rigid body accelerates, the acceleration is still unknown. But if a system of at least two rigid bodies, that are both equipped with IMUs and are connected over a joint, accelerates, then, of course, both IMUs measure the same acceleration except for the motion along the degrees of freedom of their common joint.

Given that the system of rigid bodies does not rotate, the acceleration, exerted onto the system and measured by each IMU along different axes, determines their relative orientation, as in Fig. 1.

Note that there is still no heading information for the system of rigid bodies as a whole, i.e. it is not determined whether the system faces North or East. Their relative orientation, though, is now determined except for the angle around the direction of the acceleration, which may be different from the vertical. Given that the acceleration changes direction over time, the complete relative orientation becomes observable over time. Also note that, if one is interested in the posture of a skeleton only and not in the heading of the skeleton as a whole, the relative orientations of the skeleton's bodies are sufficient.

C. Measurement Model

If the bodies do rotate, the situation is slightly more complicated due to the accelerations induced by the rotation.

The accelerations induced by rotation are different at the two accelerometers, because they are separated by a displacement which acts as an additional lever arm. To account for this, we calculate, for each rigid body of the skeleton, the accelerations virtual accelerometers positioned exactly at the joint locations would measure. For two bodies connected by a joint, the virtual accelerometers at the joint experience the same acceleration because they are at the same location, independent of the angular velocities the bodies may have.

Calculating the acceleration of a virtual accelerometer from a real accelerometer includes calculating the tangential acceleration $a_{\text{tangential}}$ over the displacement r from the real accelerometer to the joint, which is the cross-product $a_{\text{tangential}} = \dot{\omega} \times r$. The angular acceleration $\dot{\omega}$ is not measured directly. To avoid numerically differentiating the noisy gyroscope signals to obtain $\dot{\omega}$, we formulate the measurement model in terms of velocity. I.e. instead of differentiating the gyrometer measurement, we integrate the (real) accelerometer measurements.

For the bodies 1 and 2, which are part of a skeleton, are connected over a common joint and have relative orientation $Q_{1\leftarrow 2} \in \mathbb{SO}(3)$

$$v_1 + \omega_1 \times r_1 = Q_{1\leftarrow 2} (v_2 + \omega_2 \times r_2), \quad (2)$$

where v are the velocities integrated from the accelerometer measurements, ω are the angular velocities measured by the gyrometers and r are the (constant and known) displacement vectors from the IMUs to the joint location.

D. Orientation Estimation Kalman Filter

To implement the above, we use an Extended Kalman Filter [7, chapter 5] estimating the orientations of each body, where (2) replaces the magnetometer measurement model. Since body velocities are needed for (2), they join the bodies' orientations in the estimator state, such that the filter estimates the parameters of the Gaussian distribution $\mathcal{N}(X, \Sigma)$ with

$$X = \left[X^{(1)T} \dots X^{(N)T} \right]^T \quad \text{with} \quad X^{(k)} = \left[q^{(k)T} v^{(k)T} \right]^T \quad (3)$$

where $v^{(k)}$ is the k^{th} body's velocity in world coordinates, N is the number of bodies of the skeleton and $q^{(k)} \in \mathbb{R}^3$ is the scaled-axis vector parameterizing the orientation $Q^{(k)} = \text{Rot}(q^{(k)}) = \exp([q^{(k)}]_{\times}) \in \mathbb{SO}(3)$ of body k in world-coordinates. $[q]_{\times}$ turns q into the cross product matrix such that $[q]_{\times} w = q \times w$. Euler angles could be used alternatively.

Two successive filter states X_i and X_{i-1} are related by the the IMU measurements over the sampling time δt according to the dynamic model

$$\bar{X}_i = f(X_{i-1}, u_i) = \left[f'(X_{i-1}, u_i^{(k)}) \right]_{k=1}^N \quad (4)$$

with the dynamic input $u_i^{(k)} = [\omega_i^{(k)T} a_i^{(k)T}]$ consisting of the gyrometer and accelerometer measurements of the IMU attached to body k . f' updates the components of the state

concerning body k

$$f'(X_{i-1}^{(k)}, u_i^{(k)}) = \begin{bmatrix} \text{aRot} \left(\text{Rot} \left(q_{i-1}^{(k)} \right) \text{Rot} \left(\omega_i^{(k)} \delta t \right) \right) \\ v_{i-1}^{(k)} + \left(\text{Rot} \left(q_i^{(k)} \right) a_i^{(k)} + g \right) \delta t \end{bmatrix}. \quad (5)$$

Here, g is the gravitational acceleration and aRot the inverse operation to Rot . To update the covariance, we assemble from the noise densities, σ_ω and σ_a , the input's covariance

$$\Sigma_u = \begin{bmatrix} \Sigma_{u'} & & 0 \\ & \ddots & \\ 0 & & \Sigma_{u'} \end{bmatrix}, \quad \Sigma_{u'} = \begin{bmatrix} I_3 \sigma_\omega^2 / \delta t & 0 \\ 0 & I_3 \sigma_a^2 / \delta t \end{bmatrix} \quad (6)$$

and propagate it through the linearization of f with respect to the state, $A = \frac{\partial f}{\partial X_{i-1}}$, and the dynamic input, $B = \frac{\partial f}{\partial u_i}$:

$$\bar{\Sigma}_i = A \Sigma_{i-1} A^T + B \Sigma_u B^T \quad (7)$$

To compensate for accumulating drift, the measurement model of a classical orientation estimator expects the accelerometer to measure negative gravity plus noise, i.e. $-\text{Rot}(q)^T g + \delta$, $\delta \sim \mathcal{N}(0, \Sigma_\delta)$. As we have done in previous research [8], augmenting the state and dynamic model with the velocity as in (3) and (5) and using $0 = v + \delta$, $\delta \sim \mathcal{N}(0, I_3 \sigma_\delta^2)$ as a probabilistic prior also yields an orientation estimator.

To correct the relative orientations, we use (2) for all body pairs connected over a joint as a probabilistic prior. Let there be M joints. For each joint $1 \leq j \leq M$, let $p(j)$ be the body preceding and $s(j)$ succeeding the joint. Then the difference of the velocities determined by the IMUs on the bodies at joint j is

$$\left(v^{s(j)} + Q^{s(j)} \psi^{s(j)} \right) - \left(v^{p(j)} + Q^{p(j)} \psi^{p(j)} \right) = J_j \quad (8)$$

with $\psi^{(l)} = \omega^{(l)} \times r_l$ for $l = p(j), s(j)$. Because the joint can not have two different velocities at the same time, we have for all $1 \leq j \leq M$

$$J_j + \epsilon = 0 \quad \text{with } \epsilon \sim \mathcal{N}(0, I_3 \sigma_\epsilon^2). \quad (9)$$

Since (9) refers to a physical property and not to an assumption as to the system's motion, σ_ϵ^2 is much smaller than σ_δ^2 .

Over time, this determines all relative orientations of the skeleton's body, but leaves the angle around the vertical of the skeleton as a whole undetermined, because no sensor provides information about the global heading. To prevent the corresponding covariance components from growing unboundedly, we add pseudo-information. We arbitrarily pick body 1 and assume that its angle around the vertical is zero, which is equivalent to the scaled-axis parameterization of the orientation being in the horizontal plane, i.e. $q_z^{(1)} \sim \mathcal{N}(0, \sigma_z^2)$. Choosing σ_z to be very large causes the estimate to slowly drift back to zero while still following short-term gyrometer measurements.

In summary, the 'prior model' for the Kalman Filter's correction step is

$$h(X, \Omega) = \begin{bmatrix} v_{1 \dots N}^T & J_{1 \dots M}^T & q_z^{(1)} \end{bmatrix} + \zeta, \quad \zeta \sim \mathcal{N}(0, \Sigma_\zeta) \quad (10)$$

with measurements covariance

$$\Sigma_\zeta = \text{diag} \left(\overbrace{\sigma_\delta^2 \dots \sigma_\delta^2}^{N \text{ times}} \overbrace{\sigma_\epsilon^2 \dots \sigma_\epsilon^2}^{M \text{ times}} \right)$$

and the stacked current angular velocities $\Omega = [\omega_1^T \dots \omega_N^T]^T$, which are required to calculate the J_s . Using the linearizations of h ,

$$H_X = \frac{\partial}{\partial X} h \quad H_\Omega = \frac{\partial}{\partial \Omega} h \quad (11)$$

the correction of the state \bar{X} and covariance $\bar{\Sigma}$ is almost the standard linear Kalman Filter correction step:

$$K = \bar{\Sigma} H_X^T [H_X \bar{\Sigma} H_X^T + H_\Omega \sigma_\omega^2 \delta t H_\Omega^T + \Sigma_\zeta]^{-1} \quad (12)$$

$$X = \bar{X} + K(0 - h(\bar{X})) \quad (13)$$

$$\Sigma = \bar{\Sigma} - K H_X \bar{\Sigma} \quad (14)$$

In (12), $H_\Omega \sigma_\omega^2 \delta t H_\Omega^T$ enters the covariance, because h depends on the measured angular velocities. Also, (12) implies that the state, the orientations in particular, are not correlated with the current angular velocities. This obviously is an approximation, which becomes better, the more measurements are integrated between two correction steps.

E. Singularity-free Kalman Filter Implementation

The parameterizations of the orientations in our state in (3) suffer from singularities. To cure that, we use the \boxplus -theory introduced in [9], which provides the operators $\boxplus : \mathbb{S}\mathbb{O}(3) \times \mathbb{R}^3 \rightarrow \mathbb{S}\mathbb{O}(3)$ and $\boxminus : \mathbb{S}\mathbb{O}(3) \times \mathbb{S}\mathbb{O}(3) \rightarrow \mathbb{R}^3$ to apply small, vectorially represented changes to manifold elements. This practically means that we can use

$$Q_1 \boxplus \delta q = Q_1 \text{Rot}(\delta q), \quad Q_2 \boxminus Q_1 = \text{aRot}(Q_1^T Q_2) \quad (15)$$

with $Q_1, Q_2 \in \mathbb{S}\mathbb{O}(3)$, $\delta q \in \mathbb{R}^3$ to use rotation matrices and parameterize only their changes. Then (3) and (5) become

$$X = \left[X^{(1)T} \dots X^{(N)T} \right]^T \quad \text{with } X^{(k)} = \left[Q^{(k)T} v^{(k)T} \right]^T \quad (16)$$

$$f'(X_{i-1}^{(k)}, u_i^{(k)}) = \begin{bmatrix} Q_{i-1}^{(k)} \text{Rot} \left(\omega_i^{(k)} \delta t \right) \\ v_{i-1}^{(k)} + \left(Q_i^{(k)} a_i^{(k)} + g \right) \delta t \end{bmatrix}. \quad (17)$$

\boxplus and \boxminus are extended to the state component wise by

$$[Q^{(i)} v^{(i)}]_{i=1}^N \boxplus [\delta q^{(i)} \delta v^{(i)}]_{i=1}^N = [Q^{(i)} \boxplus \delta q^{(i)}, v^{(i)} + \delta v^{(i)}]_{i=1}^N$$

$$[Q_2^{(i)} v_2^{(i)}]_{i=1}^N \boxminus [Q_1^{(i)} v_1^{(i)}]_{i=1}^N = [Q_2^{(i)} \boxminus Q_1^{(i)}, v_2^{(i)} - v_1^{(i)}]_{i=1}^N.$$

That said, the linearization of the measurement model from (11) can be calculated by

$$\frac{\partial}{\partial X} h(X, \Omega) \equiv H_X = \frac{\partial}{\partial \delta x} h(X \boxplus \delta x, \Omega). \quad (18)$$

The new dynamic model linearizations, needed in (7), are

$$\frac{\partial f}{\partial X_{i-1}} \equiv A = \frac{\partial}{\partial \delta x} (f(X_{i-1} \boxplus \delta x, u_i) \boxminus f(X_{i-1}, u_i)). \quad (19)$$

B is calculated analogously. Finally we need to use \boxplus to correct the state in (13), such that it becomes

$$X = \bar{X} \boxplus K(0 - h(\bar{X})). \quad (20)$$

III. DECOUPLING ESTIMATION AND SAMPLING RATE

Our algorithm, whose correction step ((12) to (14)) is computationally expensive due to the high dimensionality, is to be eventually run on an embedded device. For our application the required estimation rate, the expensive calculation needs to be executed with, is much lower than the sampling rate of the sensors.

So it is desirable to decouple those rates, i.e. update only every n^{th} sample, while still using every sensor sample to mitigate the information loss. We accumulate per IMU the angular velocity measurements to a relative orientation and the acceleration measurements to a relative velocity at the sensor's sampling rate. The accumulation period is $\delta T = \delta t_1 + \dots + \delta t_n$, because we use irregular sampling (otherwise this would be $\delta T = n\delta t$). Instead of the raw sensor data, we use the accumulates in the dynamic model of the estimator to update the state.

Accumulating IMU data is similar to accumulating a driving robot's odometry as a homogenous coordinate transform. Such a robot pose at step j is the matrix product of the pose from the previous step, $T_{0 \leftarrow j-1}$, and the odometry increment $T_{j-1 \leftarrow j}$: $T_{0 \leftarrow j} = T_{0 \leftarrow j-1} T_{j-1 \leftarrow j}$.

In analogy, we represent an IMU accumulate at step $j-1$ with the accumulated orientation Q and velocity v by

$$M_{0 \leftarrow j-1} = \begin{bmatrix} Q_{0 \leftarrow j-1} & v_{0 \leftarrow j-1} \\ 0 & 1 \end{bmatrix}. \quad (21)$$

An IMU increment is calculated from one sensor sample as

$$M_{j-1 \leftarrow j} = \begin{bmatrix} \text{Rot}(\omega\delta t) & \text{Rot}(\frac{1}{2}\omega\delta t)a\delta t \\ 0 & 1 \end{bmatrix}. \quad (22)$$

It is used to calculate the IMU accumulate at step j :

$$M_{0 \leftarrow j} = M_{0 \leftarrow j-1} M_{j-1 \leftarrow j} \quad (23)$$

The relative accumulate over an arbitrary number of samples, n , can be recovered from two accumulates using the inverse of M .

$$\begin{aligned} M_{j-n \leftarrow j}^{(k)} &= M_{0 \leftarrow j-n}^{(k)-1} M_{0 \leftarrow j}^{(k)} = \begin{bmatrix} Q_{j-n \leftarrow j} & v_{j-n \leftarrow j} \\ 0 & 1 \end{bmatrix} \quad (24) \\ &= \begin{bmatrix} Q_{0 \leftarrow j-n}^{(k)T} Q_{0 \leftarrow j} & Q_{0 \leftarrow j-n}^{(k)T} (v_{0 \leftarrow j}^{(k)} - v_{0 \leftarrow j-n}^{(k)}) \\ 0 & 1 \end{bmatrix} \end{aligned}$$

Note that in floating point v potentially overflows, so it must be represented by a number allowed to overflow, e.g. fixed point, and the difference in (24) must be taken before applying the rotation.

To use accumulates, the dynamic model from (17) is adjusted as follows. The dynamic input concerning body k is now $u_i^{(k)} = M_{j-n \leftarrow j}^{(k)}$ and the update function of the body k 's components is

$$\begin{aligned} \bar{X}_i^{(k)} &= f'(X_{i-1}^{(k)}, u_i^{(k)}) \\ &= \begin{bmatrix} Q_{i-1}^{(k)} Q_{j-n \leftarrow j}^{(k)} \\ v_{i-1}^{(k)} + Q_{i-1}^{(k)} v_{j-n \leftarrow j}^{(k)} + g\delta T \end{bmatrix}. \quad (25) \end{aligned}$$

A. Accumulate Covariance

Because we changed the dynamic input $u_i^{(k)}$, we also need to change the dynamic input's covariance. It would be possible to accumulate the covariance of the accumulated orientation and velocity. Reconstructing the covariance of $u_i^{(k)}$, or equivalently $M_{j-n \leftarrow j}$, from the covariances of $M_{0 \leftarrow j-n}$ and $M_{0 \leftarrow j}$ would involve multiplying a potentially overflowing quantity, corrupting the result. Instead, we approximate the covariance of $u_i^{(k)}$ directly. To this end, we assume that the uncertainty of $u_i^{(k)}$ originates uniformly from each point in time over the accumulation period δT and that there were a constant angular velocity and acceleration.

The uncertainty in the accelerometer obviously leads to an uncertainty in the velocity component of $u_i^{(k)}$. Over the accumulation interval, this is

$${}_a \Sigma_{u_i'} = \begin{bmatrix} 0 & 0 \\ 0 & I_3 \sigma_a^2 \delta T \end{bmatrix} \quad (26)$$

The contribution due to the uncertainty of the gyrometer is a little trickier. At τ , the gyro noise both adds uncertainty to the final orientation and rotates the velocity accumulated after τ . Thus, at τ , we have the additional uncertainty

$$\rho(\tau) = \sigma_\omega \begin{bmatrix} I_3 \\ [-v(1 - \frac{\tau}{\delta T})]_\times \end{bmatrix} \quad (27)$$

where v is the accumulated velocity. Integrating $\rho(\tau)\rho(\tau)^T$ over the accumulation period yields the covariance contribution due to the gyrometer uncertainty:

$$\omega \Sigma_{u_i'} = \int_0^{\delta T} \rho(\tau)\rho(\tau)^T d\tau \quad (28)$$

$$= \sigma_\omega^2 \begin{bmatrix} I_3 \delta T & [v]_\times \frac{\delta T}{2} \\ [v]_\times \frac{\delta T}{2} & [v]_\times [v]_\times \frac{\delta T}{3} \end{bmatrix} \quad (29)$$

The covariance of $u_i^{(k)}$ is the sum of the two contributions

$$\Sigma_{u'} = \omega \Sigma_{u_i'} + {}_a \Sigma_{u_i'} = \delta T \begin{bmatrix} I_3 \sigma_\omega^2 & \sigma_\omega^2 [v]_\times \frac{1}{2} \\ \sigma_\omega^2 [v]_\times \frac{1}{2} & \sigma_\omega^2 [v]_\times [v]_\times \frac{1}{3} + I_3 \sigma_a^2 \end{bmatrix} \quad (30)$$

The remainder of the covariance propagation through the decoupled dynamic model is analogous to (6) and (7), the correction step remains unchanged.

IV. EXPERIMENTS AND RESULTS

To evaluate our algorithm, we built a model skeleton of three rigid bodies connected by two ball-and-socket joints. For ground truth data, we used a commercial tracking system² to observe markers which have been screwed on the rigid bodies. On each body, we mounted one of our SIRKA IMU boards using double-faced tape. Fig. 2 pictures the setup. The displacement vectors to the joints were measured manually. Since accelerometer and gyrometer bias are not part of the estimator state, both have been calibrated in advance. They could be included in the estimator state for long-term stability. To provide the motion the orientations

²ARTTrack/Dtrack2 from A.R.T. GmbH

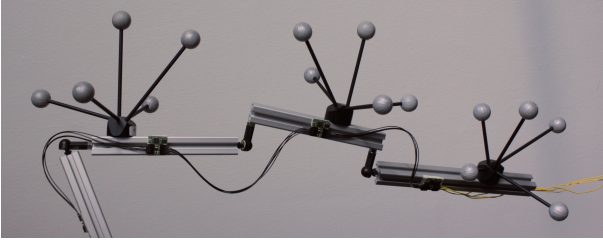


Fig. 2. The model skeleton used during the experiments. Spherical markers to be observed by the camera system are mounted on three bodies connected by ball-and-socket joints, each also carrying one SIRKA sensor board.

are to be determined from, the skeleton arm was picked up from the ground and moved around for a few seconds.

Due to the SIRKA architecture, the sensors do not operate at a constant sampling frequency and are not electrically synchronized with the camera tracking system. They are synchronized among each other, though. Each sensor board is equipped with a Bosch BMX055 IMU and a microcontroller sharing a data bus with the other sensor boards.

We have synchronized with the ground truth by correlating angular velocity norms from the gyroscope and the camera tracking system.

Both without and with rate decoupling, we tested for two properties. First, for a single body, the estimated orientation should be approximately the orientation observed by the tracking system, except for the unobservable angle around the vertical axis. Second, after the skeleton arm started to be moved, the estimates of the two relative orientations between pairs of connected bodies should be approximately the relative orientations observed using the camera tracking system.

To check the absolute orientation, we took both the estimate from IMU data, ${}^I Q_2$, and the ground truth orientation from the camera system, ${}^A Q_2$, and factored each rotation matrix into the part around the vertical axis, Q_{2z} , and around the horizontal axis, Q_{2xy} , such that

$${}^I Q_2 = {}^I Q_{2z} {}^I Q_{2xy} \quad \text{and} \quad {}^A Q_2 = {}^A Q_{2z} {}^A Q_{2xy}. \quad (31)$$

Since there is no sensor information going into ${}^I Q_{2z}$, ${}^I Q_{2z}$ and ${}^A Q_{2z}$ may differ arbitrarily. ${}^I Q_{2xy}$ and ${}^A Q_{2xy}$ should be approximately the same.

The relative orientations were computed over the connecting joints, both from IMU and ground truth,

$$\begin{aligned} {}^I Q_{1\leftarrow 2} &= {}^I Q_1^T {}^I Q_2, & {}^I Q_{2\leftarrow 3} &= {}^I Q_2^T {}^I Q_3, \\ {}^A Q_{1\leftarrow 2} &= {}^A Q_1^T {}^A Q_2, & {}^A Q_{2\leftarrow 3} &= {}^A Q_2^T {}^A Q_3. \end{aligned} \quad (32)$$

A. Results without rate decoupling

We first calculated the quantities from (31) and (32) using the estimator without rate decoupling, obtaining estimates for each IMU measurement. This took the highly unoptimized MATLAB implementation of the estimator 633 seconds. Each estimate was associated with the ground truth datum closest in time according to the previously calculated time delay.

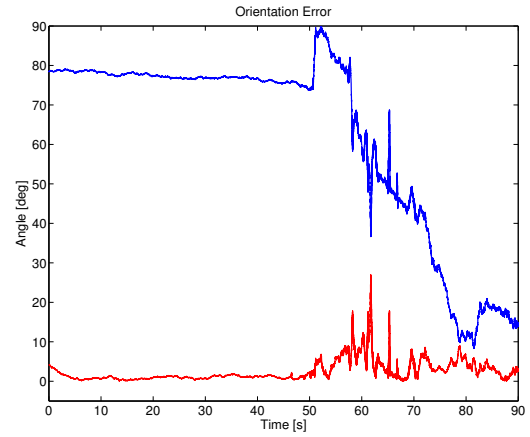


Fig. 3. Orientation error without rate decoupling. The red graph shows the error around the world-horizontal axis, the blue graph the error around the vertical axis. The latter is coincidental and depends on the motion, because there's no sensor information available about this axis.

For the orientation error, we plotted e_z and e_{xy} , such that

$$e_z = \|q_z\| \text{ s.t. } \text{Rot}(q_z) = {}^A Q_{2z}^T {}^I Q_{2z}, \quad (33)$$

$$e_{xy} = \|q_{xy}\| \text{ s.t. } \text{Rot}(q_{xy}) = {}^A Q_{2xy}^T {}^I Q_{2xy}. \quad (34)$$

The plot of Fig. 3 shows that the error around the vertical (blue) is arbitrary and depends on the motion. The skeleton arm rests on the ground for the first 50 seconds and while it does so, the error around the vertical does not change. The orientation error around the horizontal axis (red) is reasonably low while the skeleton rests and increases slightly as the skeleton is moved. The peaks appearing at around a minute are probably due to bad synchronization.

To determine the posture, the relative orientations of the bodies to each other are more interesting, and so are their errors. We calculated the relative orientation errors for the two joints analogously to (34), i.e. the errors about the first and second joint are

$$e_{\text{Joint1}} = \|q_{1\leftarrow 2}\| \text{ s.t. } \text{Rot}(q_{1\leftarrow 2}) = {}^A Q_{1\leftarrow 2}^T {}^I Q_{1\leftarrow 2} \quad (35)$$

$$e_{\text{Joint2}} = \|q_{2\leftarrow 3}\| \text{ s.t. } \text{Rot}(q_{2\leftarrow 3}) = {}^A Q_{2\leftarrow 3}^T {}^I Q_{2\leftarrow 3}. \quad (36)$$

The errors are plotted in Fig. 4. While the skeleton arm is at rest, the orientation errors stay approximately constant. As in Fig. 3, the beginning of the motion is visible. In the first 10 seconds of movement, the orientation estimates for both joints are particularly bad. After about 10 seconds the estimator gets the orientation errors for both joints below 5 degrees. This rather long settle period may be caused by linearization with the large angular error of 20° .

B. Results with rate decoupling

To see how our rate decoupling technique affects the estimates, we used the same measurement series to feed three accumulators that implement (22) and (23). At every $(n = 10)^{\text{th}}$ measurement, we used the current accumulate $M_{0\leftarrow 10k}$ to update the estimator with rate decoupling to obtain the k^{th} estimate. Thus, the estimation frequency is 10 times lower than the sampling frequency. This took an again

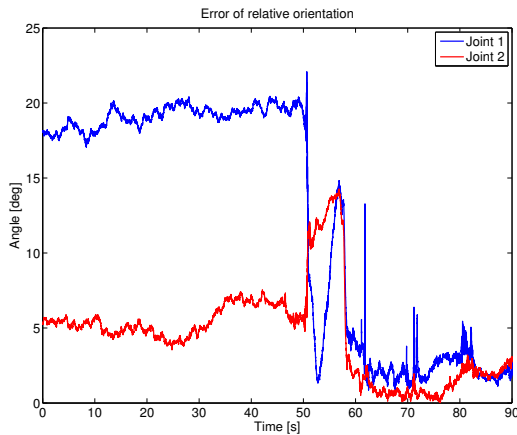


Fig. 4. Errors of the relative orientations over joint 1 (blue) and joint 2 (red). After 50 seconds, the skeleton arm starts moving, after 60 seconds the orientation error drops considerably.

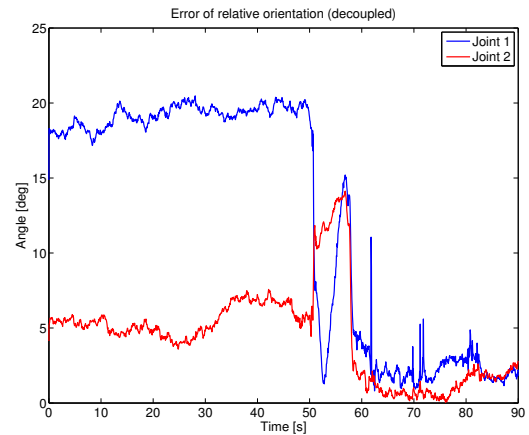


Fig. 6. Errors of the relative orientations estimated with rate decoupling over joint 1 (blue) and joint 2 (red). The errors show the same characteristics as the errors without rate decoupling plotted in Fig. 4.

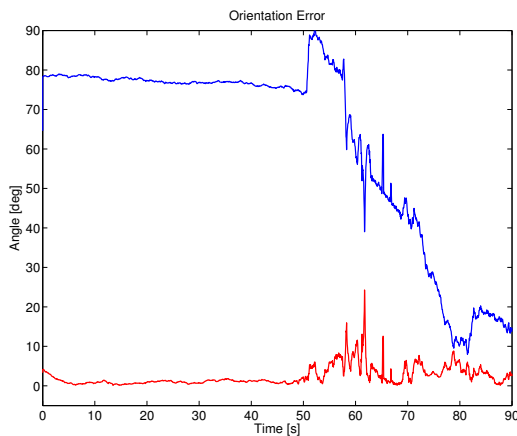


Fig. 5. Orientation error with rate decoupling. The red graph shows the error around the world-horizontal axis, the blue graph the error around the vertical axis. The error is almost identical to the error of the estimator without rate decoupling.

highly unoptimized MATLAB implementation 73 seconds, i.e. it was 8.6 times faster.

Fig. 5 shows the the corresponding orientation error plot which should be approximately the orientation error obtained without rate decoupling. And indeed, Figs. 5 and 3 look almost identical. The same is true for the more interesting errors of the relative orientations over the two joints, plotted in Fig. 6, which again looks almost identical to the plot of the errors without rate decoupling, Fig. 5. So if the required estimation rate is only $\frac{1}{10}$ of the sampling rate, there seems to be no obvious downside to using rate decoupling. To see the relative orientations themselves instead of the errors w.r.t. ground truth, watch the accompanying video.³

V. CONCLUSION

It appears that as long as the acceleration changes occasionally, magnetometer data is not necessary to determine the relative orientations of the skeleton's bodies, i.e. its posture.

³http://www.informatik.uni-bremen.de/agebv/downloads/videos/wenk_iros_15.mp4

Future research will include scaling our method from the three-body model skeleton to a larger model of a human skeleton and adding different priors – not all human joints are best approximated by ball-and-socket joints – to the correction step. Since all the sensors are supposed to be integrated into clothing, we also need to evaluate how the estimates will be affected by the sensors not being directly strapped onto the individual bodies.

Moreover, an optimized implementation tailored to the embedded hardware will replace the MATLAB program to evaluate whether the algorithm needs further modification for real-time estimation. We will also evaluate how much the estimation rate may be reduced without affecting the estimation quality of common human motion patterns.

REFERENCES

- [1] R. Ellegast, I. Hermanns, and C. Schiefer, "Workload assessment in field using the ambulatory cuela system," in *Digital Human Modeling*, ser. Lecture Notes in Computer Science, V. Duffy, Ed. Springer Berlin Heidelberg, 2009, vol. 5620, pp. 221–226.
- [2] N. Vignais, M. Miezal, G. Bleser, K. Mura, D. Gorecky, and F. Marin, "Innovative system for real-time ergonomic feedback in industrial manufacturing," *Applied Ergonomics*, vol. 44, no. 4, pp. 566 – 574, 2013.
- [3] C. M. Brigante, N. Abbate, A. Basile, A. C. Faulisi, and S. Sessa, "Towards miniaturization of a mems-based wearable motion capture system," *Industrial Electronics, IEEE Transactions on*, vol. 58, no. 8, pp. 3234–3241, 2011.
- [4] D. Roetenberg, H. Luinge, and P. Slycke, "Xsens mvn: full 6dof human motion tracking using miniature inertial sensors," Xsens Motion Technologies BV, Tech. Rep., 2009.
- [5] R. E. Kalman, "A new approach to linear filtering and prediction problems," *Journal of Fluids Engineering*, vol. 82, no. 1, pp. 35–45, 1960.
- [6] E. Kraft, "A quaternion-based unscented Kalman filter for orientation tracking," in *Proceedings of the Sixth International Conference of Information Fusion*, vol. 1, 2003, pp. 47–54.
- [7] Y. Bar-Shalom, T. Kirubarajan, and X.-R. Li, *Estimation with Applications to Tracking and Navigation*. New York, NY, USA: John Wiley & Sons, Inc., 2002.
- [8] F. Wenk and U. Frese, "Pose Estimation from Inertial Sensor Data and Prior Information," in preparation.
- [9] C. Hertzberg, R. Wagner, U. Frese, and L. Schröder, "Integrating Generic Sensor Fusion Algorithms with Sound State Representations through Encapsulation of Manifolds," *Information Fusion*, vol. 14, no. 1, pp. 57 – 77, 2013.